ARTICLE

doi:10.1038/nature11160

# Anhedonia requires MC4R-mediated synaptic adaptations in nucleus accumbens

Byung Kook Lim[1], Kee Wui Huang[1], Brad A. Grueter[1], Patrick E. Rothwell[1] & Robert C. Malenka[1]

**Chronic stress is a strong diathesis for depression in humans and is used to generate animal models of depression. It commonly leads to several major symptoms of depression, including dysregulated feeding behaviour, anhedonia and behavioural despair. Although hypotheses defining the neural pathophysiology of depression have been proposed, the critical synaptic adaptations in key brain circuits that mediate stress-induced depressive symptoms remain poorly understood. Here we show that chronic stress in mice decreases the strength of excitatory synapses on D1 dopamine receptor-expressing nucleus accumbens medium spiny neurons owing to activation of the melanocortin 4 receptor. Stress-elicited increases in behavioural measurements of anhedonia, but not increases in measurements of behavioural despair, are prevented by blocking these melanocortin 4 receptor-mediated synaptic changes *in vivo*. These results establish that stress-elicited anhedonia requires a neuropeptide-triggered, cell-type-specific synaptic adaptation in the nucleus accumbens and that distinct circuit adaptations mediate other major symptoms of stress-elicited depression.**

The neural mechanisms governing food intake have been studied extensively and a host of genetic and environmental factors influence this behaviour, mostly by affecting the levels of neuropeptides that act on the hypothalamic circuitry[1–3]. In addition, there are strong links between brain circuits mediating feeding behaviour and those responsible for appetitive motivation and 'reward', as evidenced, for example, by the simple fact that the palatability and reward value of food are influenced greatly by satiety perception[1–5]. Although two common symptoms of depression—dysregulated feeding behaviour and anhedonia—probably involve maladaptive integration and functioning of these brain circuits[1–3,6], the mechanisms by which neuropeptides that regulate food intake contribute to symptoms of depression are poorly understood.

A key brain region regulating feeding behaviour and energy homeostasis in response to metabolic rates and emotional status is the arcuate nucleus (ARC) of the hypothalamus[1–3]. It contains two major subpopulations of neurons that secrete orexigenic or anorexigenic neuropeptides, including neuropeptide Y or α-melanocyte-stimulating hormone (α-MSH), respectively. Research into the role of such neuropeptides in feeding behaviour has focused mainly on hypothalamic circuitry, whereas their actions in circuits mediating appetitive motivation are less well understood. Here, we explore the role of α-MSH signalling in the nucleus accumbens (NAc), a key component of the reward circuitry of the brain[4,5], in chronic stress-elicited behavioural changes that are commonly used as indices of depression in rodents. We focused on the potential role of α-MSH acting specifically in the NAc in mediating stress-induced depression symptoms because ARC neurons expressing α-MSH are activated by stress[7], the melanocortin 4 receptor (MC4R) is expressed in the NAc[8] and pharmacological inhibition of MC4R influences a variety of stress-induced behaviours related to anxiety, addiction and depression[8–10].

## α-MSH decreases synaptic strength in NAc D1-MSNs

To test whether α-MSH influences synaptic function in the NAc, we applied α-MSH to mouse NAc slices and examined excitatory synaptic transmission using slices prepared from bacterial artificial chromosome (BAC) transgenic mice expressing tdTomato in D1 dopamine receptor-expressing medium spiny neurons (D1-MSNs) and enhanced green fluorescent protein (eGFP) in D2 dopamine receptor-expressing MSNs (D2-MSNs; Fig. 1a)[11]. These MSN subtypes have distinct properties[12,13] and different roles in reward-related learning[14,15]. The paired-pulse ratios of excitatory postsynaptic currents (EPSCs), which inversely correlate with neurotransmitter-release probability, were not affected by α-MSH in either D1- or D2-MSNs (Supplementary Fig. 1). By contrast, a measure of changes in postsynaptic function—the ratio of the amplitude of AMPA (α-amino-3-hydroxy-5-methyl-4-isoxazolepropionic acid) receptor-mediated EPSCs to NMDA (*N*-methyl-D-aspartate) receptor-mediated EPSCs (AMPAR/NMDAR ratio)[16]—was decreased by α-MSH in D1-MSNs (Fig. 1b, c) but not in D2-MSNs (Fig. 1d, e). AMPAR-mediated miniature EPSC (mEPSC) frequency was unaffected by α-MSH but the mEPSC amplitude was decreased (Fig. 1f–i), suggesting that α-MSH caused a change in the number and/or biophysical properties of synaptic AMPARs.

Because the stoichiometry of AMPARs in NAc MSNs can be modulated by withdrawal from cocaine[17], we examined whether α-MSH influenced the voltage dependence of AMPAR EPSCs, which is an indication of the relative proportion of GluA2 (also known as GRIA2)-containing and -lacking AMPARs, as the latter AMPARs show inward rectification[18]. Although AMPAR EPSCs in control D1-MSNs showed linear current–voltage relationships, AMPAR EPSCs in D1-MSNs exposed to α-MSH showed inward rectification (Fig. 1j). This suggests that α-MSH caused an increase in the proportion of synaptic AMPARs lacking a GluA2 subunit compared with GluA2-containing AMPARs. To test this conclusion, we applied 1-naphthylacetylspermine (NASPM, 200 μM), a selective blocker of GluA2-lacking AMPARs. This manipulation had minimal effects on AMPAR EPSCs in control D1-MSNs but caused a ~50% decrease in AMPAR EPSCs in D1-MSNs that had been exposed to α-MSH (Fig. 1k). By contrast, α-MSH did not affect the stoichiometry of synaptic AMPARs in D2-MSNs (Fig. 1l, m). These results suggest that α-MSH causes a greater loss of GluA2-containing AMPARs from synapses on D1-MSNs relative to any pre-existing GluA2-lacking synaptic AMPARs. Alternatively, endocytosed GluA2-containing

[1]Nancy Pritzker Laboratory, Department of Psychiatry and Behavioral Sciences, Stanford University School of Medicine, 265 Campus Drive, Stanford, California 94305, USA.

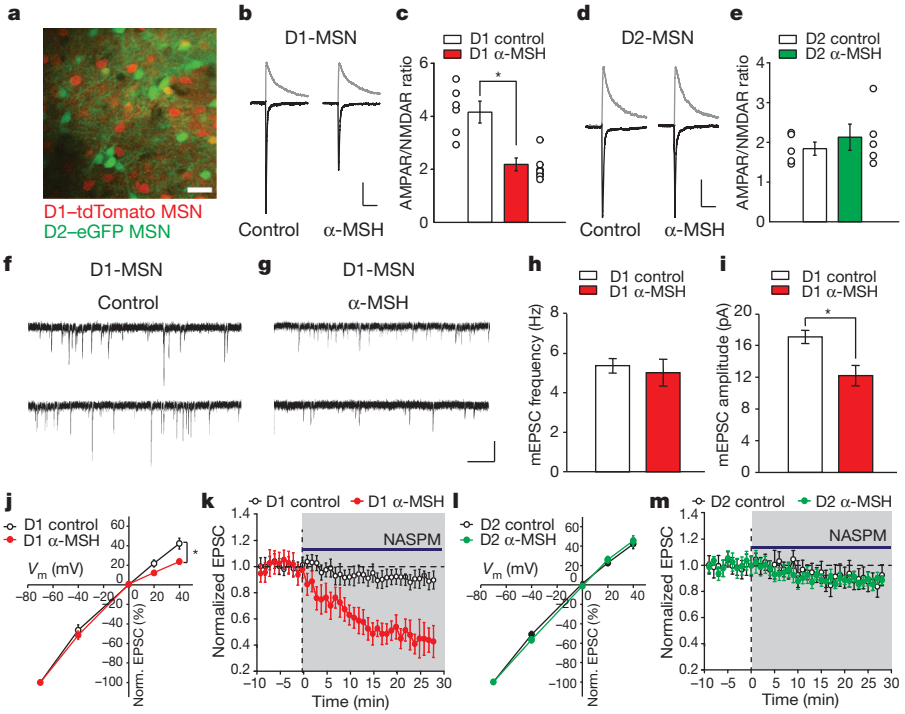


**Figure 1 | α-MSH modifies excitatory synapses on NAc D1-MSNs.** **a**, Image of an NAc slice from a D1–tdTomato and D2–eGFP BAC transgenic mouse. Scale bar, 50 μm. **b**, **c**, D1-MSN EPSCs at −70 mV and +40 mV (**b**) and summary (**c**) of α-MSH effects on AMPAR/NMDAR ratios (control, 4.16 ± 0.35, $n = 7$; α-MSH, 2.18 ± 0.29, $n = 8$). Scale bars, 60 pA (left trace), 70 pA (right trace), 100 ms. **d**, **e**, EPSCs from D2-MSNs (**d**) and summary (**e**) showing no effect of α-MSH (control, 1.86 ± 0.25, $n = 6$; α-MSH, 2.12 ± 0.34, $n = 5$). Scale bars, 90, 100 pA, 100 ms. **f**, **g**, mEPSCs from control D1-MSN (**f**) and D1-MSN exposed to α-MSH (**g**). Scale bars, 20 pA, 0.5 s. **h**, **i**, Summary of α-MSH effects on mEPSC frequency (**h**; control, 5.3 ± 0.4 Hz, $n = 9$; α-MSH, 5.0 ± 0.7 Hz, $n = 11$) and amplitude (**i**; control, 17.1 ± 0.8 pA; α-MSH, 12.2 ± 1.2 pA). **j**–**m**, Effects of α-MSH on AMPAR stoichiometry. AMPAR EPSC amplitudes at different membrane potentials (normalized to −70 mV) show that α-MSH increases AMPAR EPSC rectification in D1-MSNs (**j**; control, $n = 9$; α-MSH, $n = 12$) and enhances effects of NASPM (200 μM) (**k**; control: 89 ± 4%, $n = 6$; α-MSH: 47 ± 9% of baseline 20–25 min after NASPM application, $n = 8$). In D2-MSNs α-MSH does not affect AMPAR EPSC rectification (**l**, control, $n = 8$; α-MSH, $n = 8$) or NASPM-induced depression (**m**; control, 91 ± 5%, $n = 6$; α-MSH, 90 ± 4%, $n = 7$). Error bars denote s.e.m. $^*P < 0.05$, Mann–Whitney *U*-test.

AMPARs may have been replaced by GluA2-lacking AMPARs, but this exchange could not be one-for-one because GluA2-lacking AMPARs have a higher conductance than GluA2-containing AMPARs[18]. The cell-type-specific effects of α-MSH are consistent with the preferential expression of MC4R in D1-MSNs[8]. Differences in dopamine receptor expression between D1- and D2-MSNs are not important for the cell-type-specific actions of α-MSH because incubation of slices with D1 and D2 receptor antagonists (SCH23390 (5 μM) and raclopride (5 μM), respectively) had no effect on the decrease in AMPAR/NMDAR ratios elicited by α-MSH in D1-MSNs (control cells, $n = 5$; α-MSH-treated cells, $n = 5$; data not shown).

## Stress decreases synaptic strength in D1-MSNs via MC4R

Brain regions involved in feeding behaviour, including the lateral hypothalamus and ARC, send projections to the NAc[19]. However, the specific hypothalamic cell populations that project to the NAc have not been identified definitively. To determine whether α-MSH-expressing ARC neurons send axons to the NAc, we generated rabies viruses in which the glycoprotein was replaced by fluorophores including eGFP (RV–eGFP) and tdTomato (RV–tdTomato). These viruses are taken up by presynaptic terminals and retrogradely transported to somas where they are transduced but cannot be passed onto other synaptically connected neurons[20]. Thus, they specifically label neurons that send axonal projections directly to the site of injection (Supplementary Fig. 2). Injection of RV–eGFP into the NAc core and RV–tdTomato into the dorsal striatum resulted in robust eGFP expression in ARC neurons but no tdTomato expression (Fig. 2a). Immunostaining for α-MSH showed that a subpopulation of eGFP-expressing ARC neurons expressed α-MSH (Fig. 2b and Supplementary Fig. 3). These results demonstrate that a population of α-MSH-expressing neurons in the ARC project directly to the NAc.

Depression commonly affects appetite and MC4R antagonists ameliorate stress-induced symptoms of depression in rodents[9,10]. Furthermore, chronic-restraint stress increases the number of FOS-positive ARC neurons, which produce α-MSH[7]. Therefore, we proposed that stress-induced increases in α-MSH and MC4R signalling in NAc D1-MSNs would cause synaptic adaptations that perturb the rewarding value of food and thus are important for mediating changes in appetite during chronic stress. An 8-day restraint stress decreased body weight (Fig. 2c) owing to decreased food intake (Supplementary Fig. 4), and elicited an increase in NAc MC4R levels (Fig. 2d, e). Recordings from NAc slices prepared from chronically stressed animals showed that D1-MSN AMPAR/NMDAR ratios were decreased compared with those from non-stressed animals (Fig. 2f, g), whereas AMPAR/NMDAR ratios in D2-MSNs were unaffected by chronic stress (Fig. 2h, i). Furthermore, D1-MSN AMPAR EPSCs in slices from stressed animals showed inward rectification (Fig. 2j and Supplementary Fig. 5) and were decreased by NASPM (Fig. 2k), whereas D2-MSN AMPAR EPSCs showed minimal rectification and minimal sensitivity to NASPM (Fig. 2l, m). Thus, the synaptic adaptations in NAc MSNs caused by chronic stress mimic precisely those caused by α-MSH application.

To test directly whether α-MSH signalling through activation of MC4R mediated the synaptic changes and weight loss caused by chronic-restraint stress we generated a short hairpin RNA (shRNA) to *Mc4r* (Supplementary Fig. 6) and expressed it *in vivo* in NAc MSNs using an adeno-associated virus (AAV)-*Mc4r* shRNA (Fig. 3a, b).

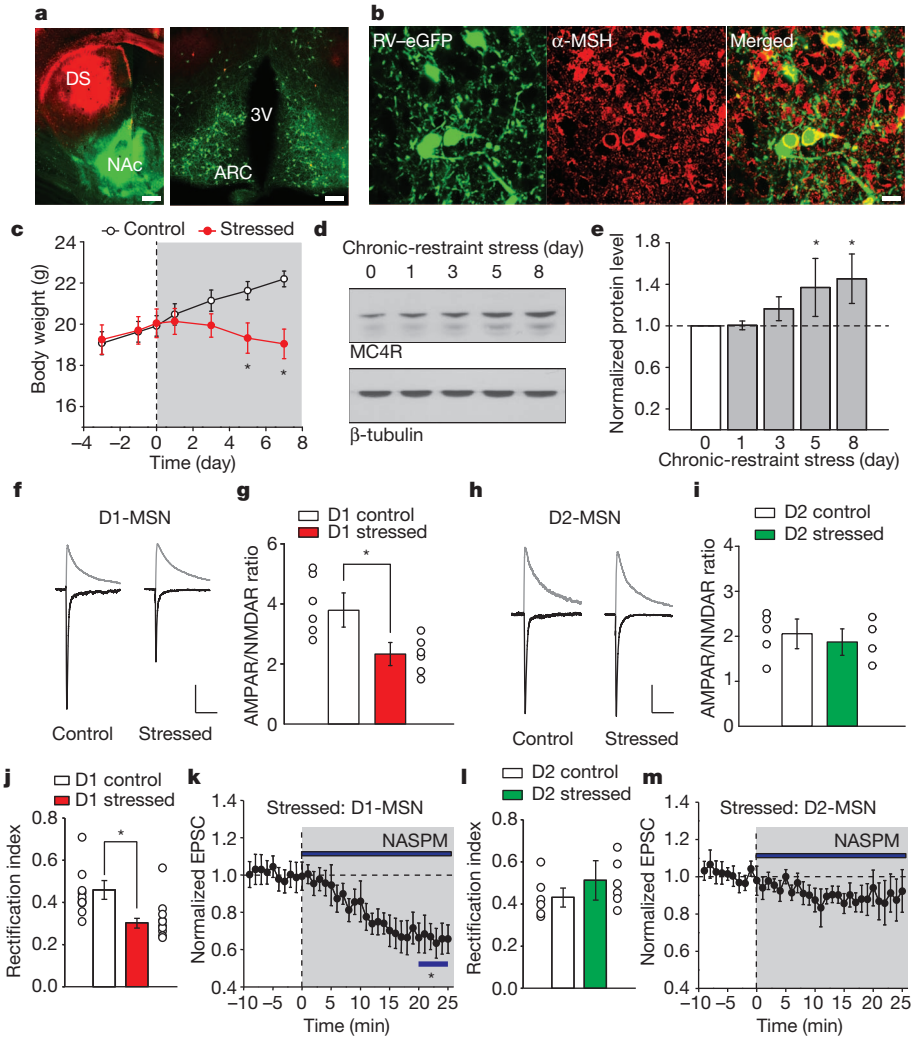


**Figure 2 | Chronic-restraint stress modifies excitatory synapses on NAc D1-MSNs.** **a**, Coronal sections of dorsal striatum (DS) and NAc (left; scale bar, 500 μm) and retrogradely labelled cells in the hypothalamus (right; scale bar, 200 μm) 1 week after injections of RV–eGFP into the NAc and RV–tdTomato into the dorsal striatum. 3V, third ventricle. **b**, ARC neurons retrogradely labelled by RV–eGFP injected into the NAc and immunostained for α-MSH (scale bar, 20 μm). **c**, Body weight of control mice ($n = 12$) and mice subjected to restraint stress ($n = 15$). **d**, **e**, Western blots (**d**) and quantification (**e**) showing changes in MC4R levels in the NAc during restraint stress (on the eighth day of restraint stress, NAc MC4R levels are 143 ± 14% of control NAc MC4R levels, $n = 3$). **f**–**i**, Effects of restraint stress on AMPAR/NMDAR ratios in D1- and D2-MSNs. EPSCs at −70 mV and +40 mV from D1-MSNs (**f**) and summary (**g**) showing stress-induced decrease in AMPAR/NMDAR ratios (control, 3.77 ± 0.59, $n = 6$; stressed, 2.34 ± 0.36, $n = 6$). Scale bar, 80, 100 pA, 100 ms. EPSCs (**h**) and summary (**i**) of AMPAR/NMDAR ratios from D2-MSNs (control, 2.03 ± 0.32, $n = 5$; stressed, 1.88 ± 0.29, $n = 4$). Scale bar, 90, 110 pA, 100 ms. **j**–**m**, Restraint stress changes AMPAR stoichiometry in D1-MSNs but not D2-MSNs. **j**, Rectification index of AMPAR EPSCs in D1-MSNs (control, 0.46 ± 0.04, $n = 8$; stressed, 0.29 ± 0.02, $n = 10$). **k**, Effect of NASPM on D1-MSN AMPAR EPSCs from stressed animals (65 ± 8%, $n = 7$). **l**, **m**, Restraint stress has no effect on D2-MSN AMPAR EPSC rectification (control rectification index, 0.43 ± 0.04, $n = 6$; stressed, 0.51 ± 0.09, $n = 6$; NASPM sensitivity, 88 ± 11%, $n = 6$). Error bars denote s.e.m. $^*P < 0.05$, Mann–Whitney *U*-test.

This caused a robust depletion of endogenous MC4R (Fig. 3c), which effectively prevented the rectification of D1-MSN AMPAR EPSCs normally caused by α-MSH application (Fig. 3d, e). Two weeks after NAc virus injection we subjected animals to chronic-restraint stress and found that knockdown of NAc MC4R prevented weight loss and the decrease in food intake, whereas injections of a control AAV expressing GFP did not (Fig. 3f and Supplementary Fig. 4). Furthermore, the increase in rectification of D1-MSN AMPAR EPSCs caused by chronic stress did not occur in cells expressing *Mc4r* shRNA, whereas this increase still occurred in D1-MSNs infected with control AAV (Fig. 3g, h). Expression of *Mc4r* shRNA in control animals had no detectable effect on AMPAR/NMDAR ratios or AMPAR EPSC rectification (data not shown). These results demonstrate that activation of MC4R in the NAc is required for chronic-stress-induced weight loss and support the hypothesis that the MC4R-induced synaptic adaptations are also required.

## α–MSH and stress occlude LTD in NAc D1–MSNs

To test whether the decrease in AMPAR EPSCs and the change in AMPAR stoichiometry caused by α-MSH activation of MC4R in D1-MSNs are in fact required for stress-induced weight loss, it was necessary to understand the mechanisms underlying these synaptic changes. Because NMDAR-triggered long-term depression (LTD) in many cell types, including NAc MSNs, involves endocytosis of AMPARs[16,21] and because GluA2 is important for this process[22,23], we proposed that MC4R activation elicits AMPAR endocytosis and therefore reduces LTD through occlusion. Consistent with this proposal, NMDAR-dependent LTD in D1-MSNs was reduced after application of α-MSH (Fig. 4a). This form of LTD was also reduced in NAc D1-MSNs in slices prepared from chronically stressed animals, an effect that was prevented by *in vivo* knockdown of MC4R (Fig. 4b). Consistent with previous results, LTD was unaffected in D2-MSNs recorded from the same NAc slices (Fig. 4c).

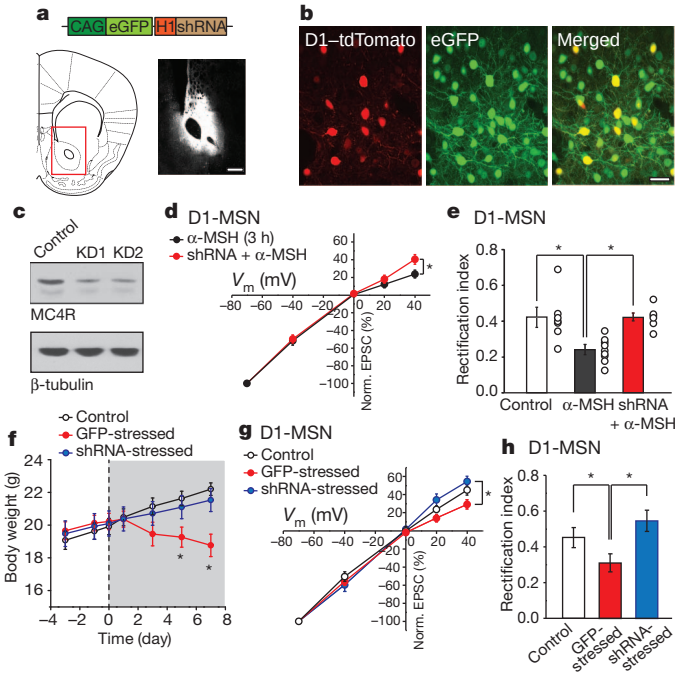


**Figure 3 | Knockdown of NAc MC4R prevents stress-induced weight loss and synaptic changes.** **a**, Schematics of AAV vector expressing *Mc4r* shRNA (top) and injection site into the NAc core (bottom left, red box, coronal section at +1.34 mm bregma) with image of eGFP expression in NAc core 2 weeks after injection (bottom right; scale bar, 500 μm). **b**, Magnified images showing eGFP expression in NAc D1–tdTomato MSNs 2 weeks after injection of AAV–*Mc4r* shRNA (scale bar, 20 μm). **c**, MC4R western blots from the NAc of two animals injected with AAV–*Mc4r* shRNA. KD, knockdown. **d**, **e**, D1-MSN AMPAR EPSC amplitudes at different membrane potentials (**d**) and rectification index (**e**, control, 0.42 ± 0.06, $n = 7$; α-MSH, 0.24 ± 0.02, $n = 9$; shRNA + α-MSH, 0.43 ± 0.02, $n = 6$) demonstrating that *in vivo Mc4r* shRNA prevents the α-MSH-induced change in D1-MSN AMPAR EPSC rectification. **f**, Stress-induced decrease in body weight is prevented by knockdown of NAc MC4R but not by injection of control AAV expressing GFP (control, $n = 12$; GFP-stressed, $n = 9$; shRNA-stressed, $n = 12$). **g**, **h**, D1-MSN AMPAR EPSC amplitudes at different membrane potentials (**g**) and rectification index (**h**, control, 0.42 ± 0.06, $n = 7$ (same as in **e**); GFP-stressed, 0.31 ± 0.05, $n = 6$; shRNA-stressed, 0.54 ± 0.08, $n = 7$), showing that *in vivo* knockdown of NAc MC4R prevents the stress-induced increase in D1-MSN AMPAR EPSC rectification. Error bars denote s.e.m. $^*P < 0.05$, Mann–Whitney *U*-test.

If MC4R activation in the NAc during chronic stress leads to synaptic modifications that are the same as those during NMDAR-dependent LTD, then LTD should be accompanied by a change in AMPAR stoichiometry. To test this prediction we induced LTD in D1-MSNs and then applied NASPM (Fig. 4d), which caused a depression of AMPAR EPSCs (Fig. 4d, e) that was similar to that caused by previous application of α-MSH (Fig. 4f). The NASPM-induced depression of AMPAR EPSCs in D1-MSNs also occurred in slices prepared from chronically stressed animals, an effect that was prevented by *in vivo* knockdown of MC4R (Fig. 4f).

The results presented thus far suggest that NMDAR-dependent LTD and the synaptic changes induced by MC4R activation are due to the endocytosis of GluA2-containing AMPARs. To test this prediction, we generated AAVs expressing a peptide based on the carboxy-terminal tail of GluA2 (G2CT-pep) that prevents the endocytosis of AMPARs (Fig. 4g)[21–23]. *In vivo* expression of this peptide strongly reduced LTD in D1-MSNs whereas expression of a control peptide did not (Fig. 4h). This peptide provided a manipulation that permitted a direct test of whether the stress-induced synaptic adaptations in D1-MSNs, like activation of MC4R, are required for the associated weight loss. Consistent with this hypothesis, expression of G2CT-pep in the NAc prevented stress-induced weight loss and a decrease in food intake, both of which occurred in animals in which the control peptide was expressed in the NAc (Fig. 4i and Supplementary Fig. 4).

Although we have demonstrated that MC4R activation in NAc D1-MSNs due to α-MSH application and chronic stress decreases AMPAR-mediated synaptic responses, these manipulations may also affect NMDARs in a manner that influences circuit function and synaptic plasticity. However, neither application of α-MSH nor chronic stress affected the time course of decay of dual-component EPSCs at +40 mV in D1-MSNs, the voltage dependence of NMDAR EPSCs or the size of NMDAR EPSCs as a function of input strength (Supplementary Fig. 7). These results demonstrate that neither α-MSH nor chronic stress detectably affect NMDAR-mediated synaptic transmission. Furthermore, the reduction of LTD in D1-MSNs by previous incubation of NAc slices with α-MSH does not require NMDAR activation (Supplementary Fig. 7).

An intriguing question is how MC4R activation causes endocytosis of GluA2-containing AMPARs. MC4R is coupled to G-protein-coupled receptors and generates increases in cyclic AMP levels[24]. Because α-MSH caused changes in synaptic AMPARs similar to those caused by activation of the cAMP-activated postsynaptic protein EPAC2 (also known as RAPGEF4) in cultured neurons[25] we examined whether application of the cAMP analogue 8-(4-chloro-phenylthio)-2′-*O*-methyladenosine-3′,5′-cyclic monophosphate (8-CPT) mimicked the synaptic effects of α-MSH. (8-CPT is used to study EPAC function because it activates EPAC but not protein kinase A[26]). Application of 8-CPT caused a decrease in the AMPAR/NMDAR ratio in D1-MSNs similar to that caused by α-MSH, as well as the same change in AMPAR stoichiometry (Supplementary Fig. 8). Furthermore, the depression of D1-MSN AMPAR EPSCs caused by 8-CPT was reduced by previous incubation of slices with α-MSH (Supplementary Fig. 8). 8-CPT application also decreased the subsequent generation of LTD (Supplementary Fig. 8). These findings suggest that α-MSH activation of MC4R in NAc D1-MSNs leads to depression of AMPAR-mediated synaptic transmission through cAMP-dependent activation of EPAC2.

## Behavioural consequences of synaptic changes in the NAc

We have presented evidence that activation of MC4R in NAc D1-MSNs and consequent synaptic adaptations are required for one major consequence of the chronic-stress protocol, anorexia leading to weight loss. Prevention of stress-induced weight loss by expression of *Mc4r* shRNA and G2CT-pep in the NAc was not due to these manipulations independently causing abnormal weight gain (Supplementary Fig. 9). To address whether behavioural manifestations of chronic stress—in particular behavioural changes used to define depression in rodents[27,28]—also require MC4R-mediated synaptic changes in D1-MSNs, we performed further depression-associated behavioural tests in control mice, mice subjected to chronic-restraint stress and chronically stressed mice in which the NAc was injected with AAVs expressing GFP, *Mc4r* shRNA, G2CT-pep or control peptide. The sucrose preference test (SPT) is a commonly used measure of anhedonia in rodent models of depression[27]. As expected, mice subjected to chronic-restraint stress showed decreased preference for the sucrose solution (Fig. 5a). This behavioural adaptation was prevented by expression of either *Mc4r* shRNA or G2CT-pep in the NAc but not by expression of GFP or control peptide (Fig. 5a). Expression of *Mc4r* shRNA in the NAc of control animals had no effect on the SPT (data not shown). These results suggest that anhedonia elicited by chronic-restraint stress, as defined by the SPT, requires the synaptic adaptations caused by MC4R activation in NAc D1-MSNs.

Notably, two other commonly used behavioural measures of 'depression' that reflect behavioural despair, the Porsolt forced-swim test and the tail-suspension test[27,28], were unaffected by the molecular manipulations that prevented stress-induced weight loss and the decrease in sucrose preference. All animals subjected to chronic-restraint stress, independent of the virus injected into NAc, showed

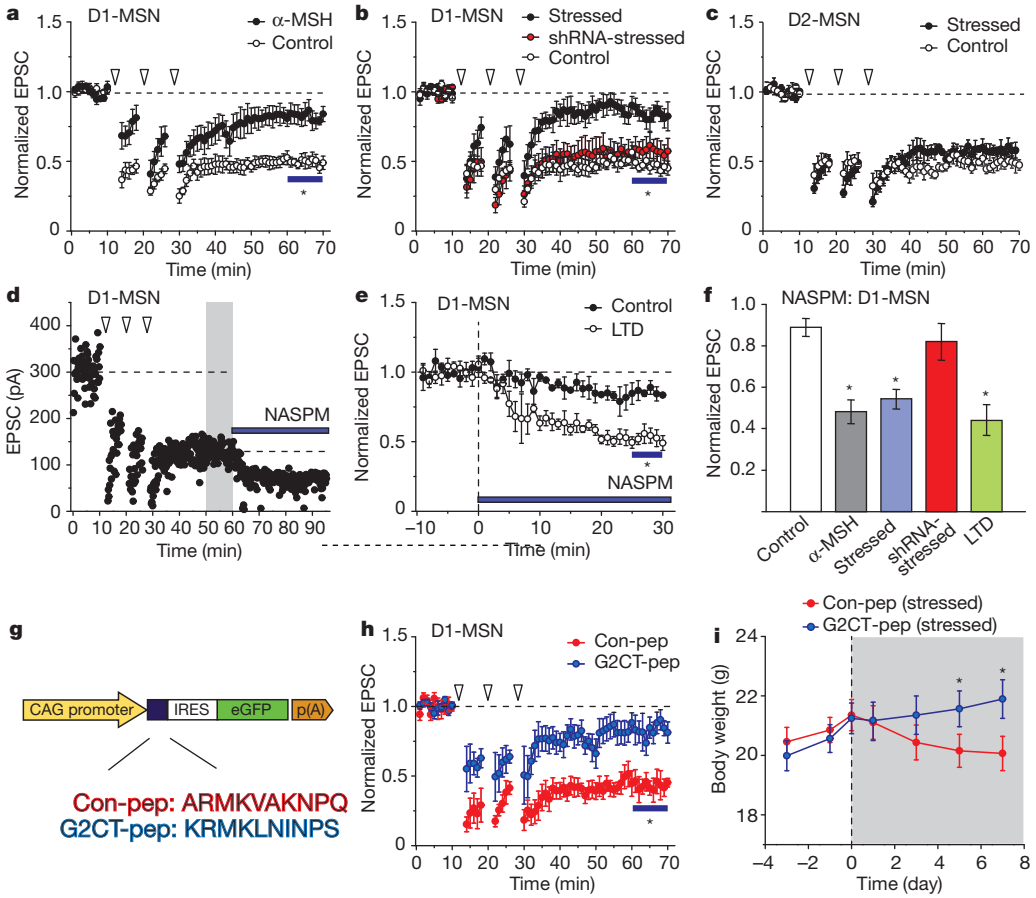


**Figure 4 | Chronic-restraint stress induces LTD in D1-MSNs. a**, Previous exposure to α-MSH reduces NMDAR-dependent LTD in NAc D1-MSNs (control, 47 ± 4% of baseline 50–60 min after start of induction protocol, $n = 7$; α-MSH, 82 ± 6%, $n = 5$). **b**, LTD in D1-MSNs is reduced by restraint stress (control, 46 ± 5%, $n = 8$; stressed, 84 ± 7%, $n = 11$) and this decrease is prevented by *in vivo* knockdown of NAc MC4R (shRNA-stressed, 0.58 ± 9%, $n = 7$). **c**, LTD in D2-MSNs is not affected by restraint stress (control, 49 ± 3%, $n = 7$; stressed, 54 ± 5%, $n = 6$). **d**, **e**, Sample experiment (**d**) and summary (**e**) showing that after LTD induction, effects of NASPM are increased (control, 85 ± 5% of baseline, $n = 6$; 51 ± 4%, $n = 4$). **f**, Effects of NASPM on D1-MSN AMPAR EPSCs after various experimental manipulations compared with control. **g**, Schematic of the AAV vector expressing control peptide (Con-pep) or a peptide blocking GluA2 binding to adaptor protein 2 (G2CT-pep). IRES, internal ribosome entry site. **h**, LTD in D1-MSNs is reduced by *in vivo* expression of G2CT-pep (81 ± 7% of baseline, $n = 6$) but not control peptide (47 ± 5%, $n = 5$). **i**, Stress-induced decrease in body weight is prevented by expression of G2CT-pep in the NAc ($n = 10$) but not by control peptide expression ($n = 9$). Error bars denote s.e.m. $^*P < 0.05$, Mann–Whitney *U*-test.

increased immobility in tail-suspension tests (Fig. 5b) as well as decreased latency to initiation of floating (Fig. 5c) and increased total time floating (Fig. 5d) in forced-swim tests. Expression of *Mc4r* shRNA in control, non-stressed animals had no significant effect on any of these behavioural measures (data not shown).

In all experiments, *Mc4r* shRNA was expressed in both D1-MSNs and D2-MSNs. Although there were no detectable synaptic effects of α-MSH or chronic stress in NAc D2-MSNs, it is conceivable that in both cell types *Mc4r* shRNA could have off-target effects that contribute to its behavioural actions. To test directly whether knockdown of only MC4R specifically in NAc D1-MSNs was responsible for reversing stress-induced weight loss and decrease in sucrose preference, we performed a cell-type-specific rescue experiment. We generated an AAV that expressed *Mc4r* shRNA together with a double-floxed, shRNA-resistant MC4R–eGFP that is only produced in cells expressing Cre recombinase (Fig. 5e). When injected into the NAc of D1-Cre mice, in which Cre recombinase is expressed only in D1-MSNs[29], robust expression of MC4R–eGFP was observed in a subpopulation of NAc cells (Fig. 5e). No expression was detected in wild-type mice injected with the same virus (Fig. 5e). The shRNA contained in this AAV was still effective in wild-type mice as evidenced by reversal of the stress-elicited weight loss (Fig. 5f) and the stress-elicited decrease in sucrose preference (Fig. 5g). By contrast, injecting this virus into the NAc of stressed D1-Cre mice resulted in behavioural measurements identical to those observed in control stressed mice (Fig. 5f, g); stressed animals showed weight loss and decreased sucrose preference. These viral-mediated molecular manipulations had no effect on stress-elicited changes in tail-suspension and forced-swim tests in either wild-type or D1-Cre mice (Fig. 5h–j).

Our results thus far suggest that the synaptic modifications in the NAc that mediate chronic stress-elicited anhedonia are different from those that mediate two behaviours that are commonly used to screen compounds for antidepressant efficacy[27,28]. However, because only a single measure of anhedonia, the SPT, was performed it is possible that the *in vivo* molecular manipulations influenced this assay solely through effects on food intake or palatability. It was therefore important to examine whether the stress protocol and our molecular manipulations affected the 'rewarding' aspect of an experience with no relationship to feeding behaviour. To accomplish this goal, we determined the dose–response function for cocaine-elicited conditioned place preference (CPP), an operational measure of an animal's experience of stimuli as 'rewarding'[30,31]. Control animals injected in the NAc with AAVs expressing GFP showed increases in the degree of CPP as a function of dose of cocaine received (Fig. 6a, b). By contrast, stressed animals that received NAc injections of the control AAV showed decreases in CPP at the lower three doses of cocaine (5, 7.5 and 10 mg kg$^{-1}$) but not at the highest dose (20 mg kg$^{-1}$) (Fig. 6a, b). These results demonstrate that stressed animals still remembered the

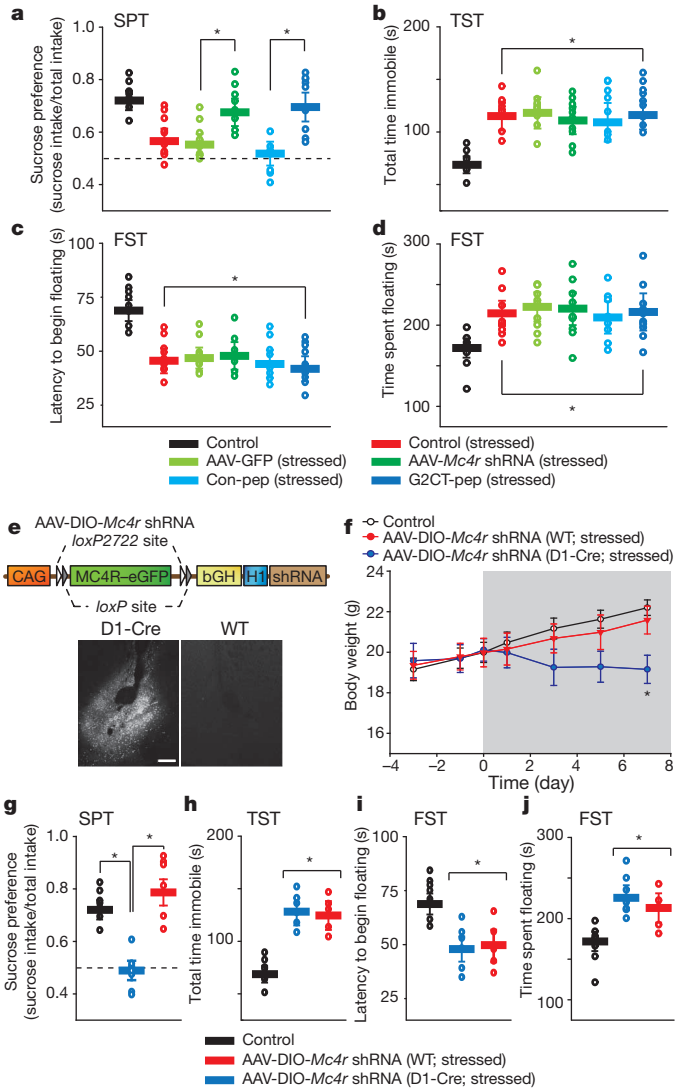


**Figure 5 | MC4R activation and LTD in the NAc are required for stress-induced anhedonia.** **a**, Summary of the SPT in control mice ($n = 9$), mice subjected to restraint stress ($n = 9$) and stressed mice that received NAc injections of AAVs expressing GFP alone ($n = 9$), *Mc4r* shRNA ($n = 10$), control peptide ($n = 8$) or G2CT-pep ($n = 10$). Expression of either *Mc4r* shRNA or G2CT-pep in the NAc prevented the stress-induced change in this test. **b**, In the tail-suspension tests, the same animals showed a stress-induced increase in time spent immobile compared with control. **c**, **d**, Animals also showed stress-induced changes in the forced swim test measured by latency to the first bout of immobile floating (**c**) or total duration of immobility/floating (**d**) compared with control. **e**. Diagram of AAV vector used to rescue MC4R in D1-MSNs only. Images of MC4R–eGFP expression after injection of virus into NAc core of D1-Cre mice and wild-type (WT) mice. Scale bar, 250 µm. bGH, bovine growth hormone polyadenylation signal. **f**. Reversal of stress-induced decrease in body weight by knockdown of NAc MC4R was prevented by D1-MSN-specific expression of shRNA-resistant *Mc4r* (control, $n = 12$; AAV-double-floxed inverted open-reading frame (DIO)-*Mc4r* shRNA (wild type), $n = 8$; AAV-DIO-*Mc4r* shRNA (D1-Cre), $n = 7$). **g–j**. Summary of the SPT (**g**), tail-suspension test (**h**) and forced-swim test (**i**, **j**) in control mice, stressed wild-type and stressed D1-Cre mice. Both groups of stressed mice received NAc injections of AAV-DIO-*Mc4r* shRNAs. D1-MSN-specific rescue of MC4R reversed the effects of *Mc4r* shRNA in the SPT but had no effect on the tail-suspension and forced-swim tests. Error bars denote s.e.m. $^*P < 0.05$, Mann–Whitney *U*-test.

context in which a strong rewarding cocaine experience occurred and therefore that the reduced CPP is due to a decreased sensitivity to cocaine reward. These stress-induced decreases in cocaine-elicited CPP were largely or entirely reversed by expression of *Mc4r* shRNA or G2CT-pep in the NAc (Fig. 6a, b).

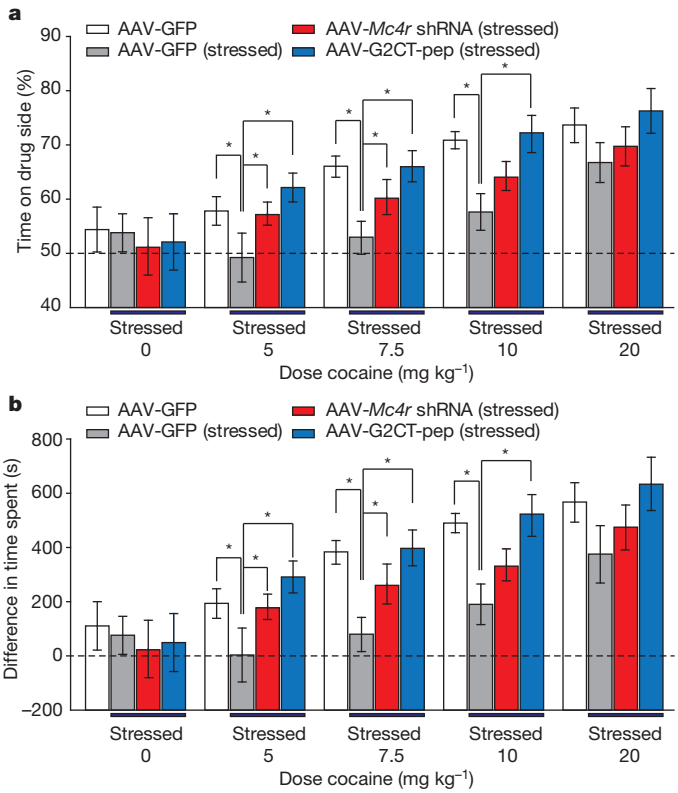


**Figure 6 | MC4R activation and LTD in the NAc are required for stress-induced decreases in cocaine CPP.** **a**, **b**, CPP induced by different doses of cocaine in mice that received NAc injection of AAV expressing GFP alone ($n = 6$), and stressed mice that received NAc injections of AAVs expressing GFP alone ($n = 6$), *Mc4r* shRNA ($n = 7$) or G2CT-pep ($n = 6$). CPP was measured as percentage of time spent on the cocaine-paired side (**a**), and the differences between time spent on cocaine-conditioned and saline-conditioned sides (**b**). Stress reduced CPP at the three lower doses but not the highest dose (20 mg kg$^{-1}$), and this decrease was prevented by expression of *Mc4r* shRNA and G2CT-pep. Error bars denote s.e.m. $^*P < 0.05$, Mann–Whitney *U*-test.

## Concluding remarks

Using complementary electrophysiological, molecular and behavioural approaches, we have presented evidence that during a chronic-stress protocol, which elicits classic behavioural manifestations of depression in rodents, activation of MC4R specifically on NAc D1-MSNs leads to a depression of excitatory synaptic transmission accompanied by a change in the stoichiometry of AMPARs, and that these synaptic adaptations are required for chronic stress-elicited anhedonia. Synaptic plasticity in the NAc, including modulation of LTD and long-term potentiation as well as changes in AMPAR stoichiometry, is important for several forms of psychostimulant-induced behavioural plasticity[17,21,32,33]. However, the synaptic properties being modified by the drug experience are temporally complex and depression-associated behavioural assays were not performed. Recently, evidence has accumulated that the two major subtypes of MSNs in both the dorsal striatum and the NAc express different synaptic properties[12,13] and participate in independent circuits mediating distinct behaviours. In the context of the present work, of greatest relevance are findings that independent modulation of D1-MSNs and D2-MSNs elicits different behavioural responses[14,15,34], which supports the hypothesis that D1-MSN activation promotes the rewarding or incentive value of cocaine whereas D2-MSN activation does the opposite. Consistent with this hypothesis, inhibition of NMDAR-mediated synaptic currents in D1-MSNs attenuated cocaine reward[35] whereas ablation of NAc D2-MSNs enhanced amphetamine CPP[36]. Assuming that activation of NAc D1-MSNs promotes the rewarding or incentive value of stimuli, our demonstration of a decrease in synaptic drive onto NAc D1-MSNs

after chronic stress makes sense as a mechanism important in contributing to anhedonia. The antidepressant effect of optogenetic activation of the medial prefrontal cortex[37], a major input to the NAc, also makes sense if this manipulation drives activity in D1-MSNs to a greater degree than D2-MSNs.

The involvement of α-MSH and MC4R signalling in NAc in triggering stress-induced synaptic adaptations provides a new molecular mechanism by which chronic stress modulates circuitry important for reward processing and incentive salience attribution[4–6,38]. Perhaps of equal importance, we have provided evidence for a dissociation between the synaptic and therefore circuit modifications required for mediating stress-elicited, depression-associated anhedonia and those that mediate changes in the forced-swim and tail-suspension tests, behaviours that are used to predict antidepressant efficacy[27,28]. Synaptic adaptations in other brain areas, such as the lateral habenula[39], may be important for these latter depression-associated behaviours. This dissociation also points out limitations of commonly used approaches to developing antidepressant medications. By delineating the molecular mechanisms underlying the circuit modifications that mediate specific behavioural manifestations of psychiatric symptoms such as anhedonia, it should be possible to accelerate the development of efficacious therapies with new mechanisms of action.

## METHODS SUMMARY

Male adult (6–9 weeks of age) C57BL/6, DRD1A–tdTomato/DRD2–eGFP BAC transgenic mice[11] backcrossed to C57BL/6 mice or DRD1A-Cre BAC transgenic mice[29] backcrossed to C57BL/6 mice were used for all experiments. All procedures complied with the animal care standards set forth by the National Institutes of Health and were approved by Stanford University's Administrative Panel on Laboratory Animal Care. Animals were subjected to chronic-restraint stress by placement for 3–4 h per day for 7–8 consecutive days in 50-ml conical tubes with holes for air flow. During the restraint stress, animals were placed in separate sound- and light-attenuating boxes and then immediately returned to their home cages. Approximately 75% of the electrophysiological assays and 70% of the behavioural assays (Figs 5 and 6) were performed blindly without knowledge of the treatment history of the animals.

**Full Methods** and any associated references are available in the online version of the paper at www.nature.com/nature.

**Received 1 November 2011; accepted 25 April 2012.**


1. Cone, R. D. Anatomy and regulation of the central melanocortin system. *Nature Neurosci.* **8,** 571–578 (2005).
2. Gao, Q. & Horvath, T. L. Neurobiology of feeding and energy expenditure. *Annu. Rev. Neurosci.* **30,** 367–398 (2007).
3. Morton, G. J., Cummings, D. E., Baskin, D. G., Barsh, G. S. & Schwartz, M. W. Central nervous system control of food intake and body weight. *Nature* **443,** 289–295 (2006).
4. Kelley, A. E. & Berridge, K. C. The neuroscience of natural rewards: relevance to addictive drugs. *J. Neurosci.* **22,** 3306–3311 (2002).
5. Volkow, N. D., Wang, G. J. & Baler, R. D. Reward, dopamine and the control of food intake: implications for obesity. *Tr. Cogn. Sci.* **15,** 37–46 (2011).
6. Nestler, E. J. & Carlezon, W. A. Jr. The mesolimbic dopamine reward circuit in depression. *Biol. Psychiatry* **59,** 1151–1159 (2006).
7. Liu, J. *et al.* The melanocortinergic pathway is rapidly recruited by emotional stress and contributes to stress-induced anorexia and anxiety-like behavior. *Endocrinology* **148,** 5531–5540 (2007).
8. Hsu, R. *et al.* Blockade of melanocortin transmission inhibits cocaine reward. *Eur. J. Neurosci.* **21,** 2233–2242 (2005).
9. Chaki, S., Ogawa, S., Toda, Y., Funakoshi, T. & Okuyama, S. Involvement of the melanocortin MC4 receptor in stress-related behavior in rodents. *Eur. J. Pharmacol.* **474,** 95–101 (2003).
10. Chaki, S. & Okuyama, S. Involvement of melanocortin-4 receptor in anxiety and depression. *Peptides* **26,** 1952–1964 (2005).
11. Shuen, J. A., Chen, M., Gloss, B. & Calakos, N. *Drd1a*-tdTomato BAC transgenic mice for simultaneous visualization of medium spiny neurons in the direct and indirect pathways of the basal ganglia. *J. Neurosci.* **28,** 2681–2685 (2008).
12. Kreitzer, A. C. & Malenka, R. C. Striatal plasticity and basal ganglia circuit function. *Neuron* **60,** 543–554 (2008).
13. Grueter, B. A., Brasnjo, G. & Malenka, R. C. Postsynaptic TRPV1 triggers cell type-specific long-term depression in the nucleus accumbens. *Nature Neurosci.* **13,** 1519–1525 (2010).
14. Lobo, M. K. *et al.* Cell type-specific loss of BDNF signaling mimics optogenetic control of cocaine reward. *Science* **330,** 385–390 (2010).
15. Hikida, T., Kimura, K., Wada, N., Funabiki, K. & Nakanishi, S. Distinct roles of synaptic transmission in direct and indirect striatal pathways to reward and aversive behavior. *Neuron* **66,** 896–907 (2010).
16. Kauer, J. A. & Malenka, R. C. Synaptic plasticity and addiction. *Nature Rev. Neurosci.* **8,** 844–858 (2007).
17. Conrad, K. L. *et al.* Formation of accumbens GluR2-lacking AMPA receptors mediates incubation of cocaine craving. *Nature* **454,** 118–121 (2008).
18. Isaac, J. T., Ashby, M. C. & McBain, C. J. The role of the GluR2 subunit in AMPA receptor function and synaptic plasticity. *Neuron* **54,** 859–871 (2007).
19. Brog, J. S., Salyapongse, A., Deutch, A. Y. & Zahm, D. S. The patterns of afferent innervation of the core and shell in the "accumbens" part of the rat ventral striatum: immunohistochemical detection of retrogradely transported fluoro-gold. *J. Comp. Neurol.* **338,** 255–278 (1993).
20. Wickersham, I. R., Finke, S., Conzelmann, K. K. & Callaway, E. M. Retrograde neuronal tracing with a deletion-mutant rabies virus. *Nature Methods* **4,** 47–49 (2007).
21. Brebner, K. *et al.* Nucleus accumbens long-term depression and the expression of behavioral sensitization. *Science* **310,** 1340–1343 (2005).
22. Shepherd, J. D. & Huganir, R. L. The cell biology of synaptic plasticity: AMPA receptor trafficking. *Annu. Rev. Cell Dev. Biol.* **23,** 613–643 (2007).
23. Lee, S. H., Liu, L., Wang, Y. T. & Sheng, M. Clathrin adaptor AP2 and NSF interact with overlapping sites of GluR2 and play distinct roles in AMPA receptor trafficking and hippocampal LTD. *Neuron* **36,** 661–674 (2002).
24. Yang, Y. Structure, function and regulation of the melanocortin receptors. *Eur. J. Pharmacol.* **660,** 125–130 (2011).
25. Woolfrey, K. M. *et al.* Epac2 induces synapse remodeling and depression and its disease-associated forms alter spines. *Nature Neurosci.* **12,** 1275–1284 (2009).
26. Bos, J. L. Epac proteins: multi-purpose cAMP targets. *Trends Biochem. Sci.* **31,** 680–686 (2006).
27. Nestler, E. J. & Hyman, S. E. Animal models of neuropsychiatric disorders. *Nature Neurosci.* **13,** 1161–1169 (2010).
28. Porsolt, R. D., Brossard, G., Hautbois, C. & Roux, S. Rodent models of depression: forced swimming and tail suspension behavioral despair tests in rats and mice. *Curr. Protoc. Neurosci.* **14,** 10A.1–8.10A.10 (2001).
29. Gong, S. *et al.* Targeting Cre recombinase to specific neuron populations with bacterial artificial chromosome constructs. *J. Neurosci.* **27,** 9817–9823 (2007).
30. Bardo, M. T. & Bevins, R. A. Conditioned place preference: what does it add to our preclinical understanding of drug reward? *Psychopharmacology* **153,** 31–43 (2000).
31. Cunningham, C. L., Gremel, C. M. & Groblewski, P. A. Drug-induced conditioned place preference and aversion in mice. *Nature Protocols* **1,** 1662–1670 (2006).
32. Kasanetz, F. *et al.* Transition to addiction is associated with a persistent impairment in synaptic plasticity. *Science* **328,** 1709–1712 (2010).
33. Pascoli, V., Turiault, M. & Luscher, C. Reversal of cocaine-evoked synaptic potentiation resets drug-induced adaptive behaviour. *Nature* **481,** 71–75 (2011).
34. Ferguson, S. M. *et al.* Transient neuronal inhibition reveals opposing roles of indirect and direct pathways in sensitization. *Nature Neurosci.* **14,** 22–24 (2011).
35. Heusner, C. L. & Palmiter, R. D. Expression of mutant NMDA receptors in dopamine D1 receptor-containing cells prevents cocaine sensitization and decreases cocaine preference. *J. Neurosci.* **25,** 6651–6657 (2005).
36. Durieux, P. F. *et al.* D2R striatopallidal neurons inhibit both locomotor and drug reward processes. *Nature Neurosci.* **12,** 393–395 (2009).
37. Covington, H. E. III *et al.* Antidepressant effect of optogenetic stimulation of the medial prefrontal cortex. *J. Neurosci.* **30,** 16082–16090 (2010).
38. Berridge, K. C., Robinson, T. E. & Aldridge, J. W. Dissecting components of reward: 'liking', 'wanting', and learning. *Curr. Opin. Pharmacol.* **9,** 65–73 (2009).
39. Li, B. *et al.* Synaptic potentiation onto habenula neurons in the learned helplessness model of depression. *Nature* **470,** 535–539 (2011).


**Supplementary Information** is linked to the online version of the paper at www.nature.com/nature.

**Acknowledgements** We thank J. Kauer, D. Lyons and members of the Malenka laboratory for comments. The rabies virus complementary DNA plasmid and viral component-expressing plasmids were gifts from K. Conzelmann and I. Wickersham. BAC transgenic mice were provided by N. Calakos. BHK-B19G cells were a gift from E. Callaway. The AAVs used in this study were produced by the Stanford Neuroscience Gene Vector and Virus Core. The AAV-DJ helper plasmid was a gift from M. Kay. B.K.L. is supported by a Davis Foundation Postdoctoral Fellowship in Eating Disorders Research. We acknowledge funding from the National Institutes of Health (R.C.M.).

**Author Contributions** The study was designed and results were interpreted by B.K.L. and R.C.M. with assistance from K.W.H., B.A.G. and P.E.R. Virus injections and rabies virus production were performed by B.K.L. and K.W.H. All experiments were performed and analysed by B.K.L. with assistance from B.A.G. for electrophysiology experiments and P.E.R. for CPP assays. The manuscript was written by B.K.L. and R.C.M. and edited by all authors.

**Author Information** Reprints and permissions information is available at www.nature.com/reprints. The authors declare no competing financial interests. Readers are welcome to comment on the online version of this article at www.nature.com/nature. Correspondence and requests for materials should be addressed to R.C.M. (malenka@stanford.edu).

## METHODS

**Animals.** Male adult (6–9 weeks of age) C57BL/6, DRD1A–tdTomato/DRD2–eGFP BAC transgenic mice[11] backcrossed to C57BL/6 mice or DRD1A-Cre BAC transgenic mice[29] backcrossed to C57BL/6 mice were used for all experiments. All procedures complied with the animal care standards set forth by the National Institutes of Health and were approved by Stanford University's Administrative Panel on Laboratory Animal Care. Animals were subjected to chronic-restraint stress by placement for 3–4 h per day for 7–8 consecutive days in 50-ml conical tubes with holes for air flow. During the restraint stress, animals were placed in separate sound- and light-attenuating boxes and then immediately returned to their home cages. Approximately 75% of the electrophysiological assays and 70% of the behavioural assays (Figs 5 and 6) were performed blindly without knowledge of the treatment history of the animals.

**Electrophysiology.** Parasagittal slices (250 μm) containing the NAc core were prepared from D1–tdTomato/D2–eGFP heterozygotic BAC transgenic mice[11] on a C57BL/6 background using standard procedures. In brief, after mice were anaesthetized with isoflurane and decapitated, brains were quickly removed and placed in ice-cold, low-sodium high-sucrose dissecting solution. Slices were cut by adhering the two sagittal hemispheres brain containing the NAc core to the stage of a Leica vibroslicer. Slices were allowed to recover for a minimum of 60 min in a submerged holding chamber (~25 °C) containing artificial cerebrospinal fluid (ACSF) consisting of 124 mM NaCl, 4.4 mM KCl, 2.5 mM $CaCl_2$, 1.3 mM $MgSO_4$, 1 mM $NaH_2PO_4$, 11 mM glucose and 26 mM $NaHCO_3$. Slices were then removed from the holding chamber and placed in the recording chamber where they were perfused continuously with oxygenated (95% $O_2$, 5% $CO_2$) ACSF at a rate of 2 ml $min^{-1}$ at 30 ± 2 °C. Picrotoxin (50 μM) was added to the ACSF to block $GABA_A$ (γ-aminobutyric acid type A) receptor-mediated inhibitory synaptic currents. Whole-cell voltage-clamp recordings from MSNs were obtained under visual control using a ×63 objective. The NAc core was identified by the presence of the anterior commissure. D1- and D2-MSNs in the NAc core were identified by the presence of tdTomato and eGFP, respectively, which were excited with ultraviolet light using bandpass filters (HQ545/×30 exciter filter (EX) for tdTomato; HQ470/×40 EX for eGFP). Recordings were made with electrodes (3.0–6.0 MΩ) filled with 120 mM $CsMeSO_4$, 15 mM CsCl, 8 mM NaCl, 10 mM HEPES, 0.2 mM EGTA, 10 mM tetraethylammonium chloride, 4 mM MgATP, 0.3 mM NaGTP, 0.1 mM spermine and 5 mM QX-314. Excitatory afferents were stimulated with a bipolar nichrome wire electrode placed at the border between the NAc core and the cortex dorsal to the anterior commissure. Recordings were performed using a multiclamp 700B (Molecular Devices), filtered at 2 kHz and digitized at 10 kHz. EPSCs of 100–400 pA were evoked at a frequency of 0.1 Hz, and MSNs were voltage-clamped at −70 mV unless otherwise stated. Data acquisition and analysis were performed online using custom Igor Pro software. Input resistance and access resistance were monitored continuously throughout each experiment; experiments were terminated if these changed by >20%.

For monitoring α-MSH-induced synaptic changes, NAc slices were incubated in ACSF containing α-MSH (1 μM) for 2–3 h before recordings were made. Acute application of α-MSH during recordings yielded, on average, insignificant synaptic changes during 30–45 min of application. Paired-pulse ratios were acquired by applying a second afferent stimulus of equal intensity at a specified time after the first stimulus and then calculating the ratio of EPSC2/EPSC1. For each cell for a given inter-stimulus interval, the pulse-paired ratios of six consecutive responses were averaged. AMPAR/NMDAR ratios were calculated as the ratio of the peak amplitude of the EPSC at −70 mV (AMPAR EPSCs) to the magnitude of the EPSC recorded at +40 mV at 50–55 ms after afferent stimulation. mEPSCs were collected at a holding potential of −70 mV in the presence of tetrodotoxin (0.5 μM). Thirty-second blocks of events were acquired and analysed using mini-analysis software (Synaptosoft) with threshold parameters set at 5 pA amplitude and <3 ms rise time. All events included in the final data analysis were verified by eye. Summary LTD graphs were generated by averaging the peak amplitudes of individual EPSCs in 1-min bins (six consecutive sweeps) and normalizing these to the mean value of EPSCs collected during the 10-min baseline immediately before the LTD-induction protocol (three bouts of 5 Hz stimulation for 3 min with 5-min intervals between bouts while holding cells at –50 mV)[40]. Individual experiments were then averaged together. For all experiments examining LTD or the effects of α-MSH incubation, recordings from control cells were interleaved with recordings from cells undergoing the experimental manipulation with a ratio of one control cell for every two to four experimental cells. Comparisons between different experimental manipulations were made using a Mann–Whitney *U*-test with $P < 0.05$ considered significant. All statements in the text about differences between grouped data indicate that statistical significance was achieved. All values are reported as mean ± s.e.m.

**Virus and shRNA generation.** The AAVs used in this study were produced by the Stanford Neuroscience Gene Vector and Virus Core. In brief, AAV-DJ[41] was produced by transfection of AAV 293 cells (Agilent) with three plasmids: an AAV vector expressing the shRNA to *Mc4r* and eGFP or eGFP alone, AAV helper plasmid (pHELPER; Agilent) and AAV rep-cap helper plasmid (pRC-DJ, gift from M. Kay). At 72 h after transfection, the cells were collected and lysed by a freeze–thaw procedure. Viral particles were then purified by an iodixanol step-gradient ultracentrifugation method. The iodixanol was diluted and the AAV was concentrated using a 100-kDa molecular mass cutoff ultrafiltration device. The genomic titre was determined by quantitative PCR. To construct shRNAs, oligonucleotides that contained 21-base sense and antisense sequences were connected with a hairpin loop followed by a poly(T) termination signal. The 21 base-pair sequence targeting *Mc4r* (GenBank accession: NM_016977) that was used in all experiments is 5′-GGAGAACATTCTAGTGATCGT-3′. This shRNA was ligated into an AAV vector expressing eGFP. For initial testing of the efficacy of the shRNA, full-length mouse *Mc4r* complementary DNA was fused to DsRed-monomer for fluorescent quantification of MC4R expression (MC4R–DsRed) in HEK293 cells. The plasmid expressing MC4R–DsRed was transfected and 3–4 h later cells were infected with AAVs expressing the *Mc4r* shRNA. Two or three days after infection, the proportion of cells expressing detectable MC4R–DsRed was determined and found to be reduced from >80% to <20% (Supplementary Fig. 4). To achieve specific MC4R expression in D1-MSNs in D1-Cre mice, we used AAV vectors with a double-floxed inverted open reading frame[42,43]. In brief, the eGFP-tagged shRNA-resistant *Mc4r* was cloned and inserted between *loxP* and *lox2722* sites in the reverse orientation. The resulting double-floxed reverse MC4R–eGFP was cloned into AAV vectors expressing *Mc4r* shRNA (Fig. 5e).

Rabies viruses were generated from a full-length cDNA plasmid containing all components of the virus (SAD L16; gift from K. K. Conzelmann)[44]. We replaced the viral glycoprotein with eGFP (RV–eGFP) or tdTomato (RV–tdTomato) to generate viruses expressing eGFP or tdTomato. To rescue rabies viruses from this cDNA we used a modified version of a published protocol[44,45]. In brief, HEK293T cells were transfected with a total of six plasmids; four plasmids expressing the viral components pTIT-N, pTIT-P, pTIT-G and pTIT-L; one plasmid expressing T7 RNA polymerase (pCAGGS-T7) and the aforementioned glycoprotein-deleted viral cDNA plasmid expressing eGFP or tdTomato. For the amplification of rabies virus, the media bathing these HEK293T cells was collected 3–4 days post-transfection and moved to BHK-B19G cells stably expressing viral glycoprotein[20]. After 3 days, the media from BHK-B19G cells was collected, centrifuged for 5 min at 3,000*g* to remove cell debris, and concentrated by ultracentrifugation (55,000*g* for 2 h). Pellets were suspended in Dulbecco's PBS, aliquoted and stored at −80 °C. The titre of concentrated virus was measured by infecting HEK293 cells and monitoring fluorescence. Plasmids expressing the viral components were gifts from K. K. Conzelmann and I. Wickersham. BHK cells stably expressing B19G were a gift from E. Callaway.

**Stereotaxic injections.** Stereotaxic injection of viruses into the NAc was performed under general ketamine–medetomidine anaesthesia using a stereotaxic instrument (David Kopf Instruments). A small volume (~500 nl) of concentrated virus solution was injected unilaterally or bilaterally into the NAc core (bregma 1.54 mm; lateral 1.0 mm; ventral 4.0 mm) or dorsolateral striatum (bregma 0.98 mm; lateral 1.8 mm; ventral 2.2 mm) at a slow rate (100 nl $min^{-1}$) using a syringe pump (Harvard Apparatus). The injection needle was withdrawn 5 min after the end of the infusion. Animals were used 2–3 weeks after AAV injections and 1 week after rabies virus injections. Injection sites were confirmed in all animals by preparing coronal sections (50–100 μm) containing the dorsal striatum and NAc.

**Immunohistochemistry.** Immunohistochemistry and confocal microscopy were performed as described previously[46]. In brief, after intracardial perfusion with 4% paraformaldehyde in PBS (pH 7.4), the brains were fixed overnight in the same solution and coronal slices (50 μm) containing the hypothalamus were prepared. To stain for α-MSH, a rabbit anti-α-MSH antibody (ImmunoStar; 1:200) was applied overnight in a solution containing 1% horse serum, 0.2% BSA and 0.5% Triton X-100 in PBS. Slices were then washed four times in PBS and incubated with an AlexaFluor568 goat anti-rabbit secondary antibody (Molecular Probes; 1:750) for 2 h in PBS containing 0.5% Triton X-100. Subsequently, slices were washed five times and mounted using vectashield mounting medium (Vector Laboratories). To identify cells expressing eGFP owing to the injection of RV–eGFP into the NAc, raw eGFP fluorescence was visualized. Image acquisition was performed with a confocal microscope (Zeiss LSM510) using a ×10/0.30 Plan-Neofluar and a ×63/1.40 oil differential interference contrast Plan Apochromat objective. Confocal images were examined using the Zeiss LSM Image Browser software.

**Behavioural assays.** Animals were weighed daily at the same time for 3 days before and throughout the restraint stress. Food intake was measured for a 24-h period on the day before the initiation of the restraint stress and the day after the

termination of the restraint stress. The Porsolt forced-swim test was based on a previously described procedure[28]. At the same time each day, mice were placed individually in glass cylinders that were filled with water (25 °C) to a depth that was sufficient to prevent mice from supporting themselves by placing their tails on the base of the cylinder. Each session was videotaped for offline analyses and the water was changed between sessions. Immobility was defined as the lack of any swimming movements for >10 s. The latency to the first bout of immobility and the duration of immobility for the last 4 min of the total 6-min test period were measured.

The tail-suspension test was based on a previously described procedure[28]. In brief, each mouse was individually suspended 20 cm above the floor with adhesive tape placed 1 cm from the tip of the tail. Animals were considered to be immobile when they exhibited no body movement and hung passively for >10 s. The time during which mice remained immobile was quantified over a period of 6 min.

For the SPT, two water bottles were attached to cages housing individual mice. For the first 24 h, both bottles contained water. The next day, one bottle was filled with water containing 2% sucrose and the total volume of liquid consumed from each bottle over the ensuing 24 h was measured. The sucrose preference was calculated as the fraction of sucrose solution consumed compared to the total amount of solution consumed from both bottles. Bottles containing the sucrose solution were randomly placed on the left or right side of the compartment.

CPP was conducted based on previously described procedures[31] using an open-field activity chamber (ENV-510, Med Associates) equipped with infrared beams and a software interface (activity monitor, Med Associates) that monitored the position of the mouse[13]. The apparatus was divided into two equally sized zones using plastic floor tiles with distinct visual and tactile cues (grey and smooth or white and rough). The amount of time spent freely exploring each zone was recorded during 20-min test sessions. After an initial test to establish baseline preference for the two sets of cues, each mouse was randomly assigned in a counterbalanced fashion to receive cocaine in the presence of one set of cues (that is, an unbiased design). Four conditioning cycles were conducted with ascending doses of cocaine (5, 7.5, 10 and 20 mg $kg^{-1}$). Each cycle began with an intraperitoneal injection of saline and exposure to the appropriate set of cues for 20 min. A second conditioning session with cocaine was conducted 2–4 h later in the presence of the other set of cues. A test session was conducted the day after conditioning to determine time spent in the presence of the cocaine-associated cues (that is, CPP), and the next cycle of conditioning commenced the next day. This protocol allowed us to determine a dose–response function for cocaine CPP in each individual subject, providing enhanced resolution for detecting shifts in cocaine sensitivity caused by stressful experience and viral-mediated molecular manipulations.

**Measurement of MC4R expression in the NAc.** NAc tissue surrounding the anterior commissure was dissected from freshly isolated brain slices and frozen rapidly in liquid nitrogen. This tissue was then lysed in ice-cold homogenate buffer (50 mM Tris-HCl, 150 mM NaCl, Nonidet P40, 0.5% sodium deoxycholate, pH 7.5) containing a protease-inhibitor cocktail (Roche Applied Science) and homogenized. The protein concentration of the lysates was measured using the Bradford method (Bio-Rad) and 50 μg of lysates was used for analysis. Samples were separated on 4–12% gradient Bis–Tris gels (Invitrogen) and transferred onto nitrocellulose membranes. After transfer, the membranes were blocked with 5% milk in 0.1 M PBS and incubated overnight at 4 °C with rabbit polyclonal MC4R antibody (Abcam) or mouse monoclonal β-tubulin antibody (Abcam). After washing five times with PBS containing 0.5% Tween20, the membrane was incubated with horseradish peroxidase-conjugated anti-rabbit or anti-mouse secondary antibody (1:5,000, Sigma) for 1 h. The immune-reactive bands were visualized using an ECL chemiluminescence reagent (GE Healthcare) according to the manufacturer's instructions. The scanned digital images were used for quantification. For comparing the levels of MC4R, the intensity of MC4R signals was normalized to the intensity of the β-tubulin signal.


40. Thomas, M. J., Beurrier, C., Bonci, A. & Malenka, R. C. Long-term depression in the nucleus accumbens: a neural correlate of behavioral sensitization to cocaine. *Nature Neurosci.* **4,** 1217–1223 (2001).
41. Grimm, D. *et al. In vitro* and *in vivo* gene therapy vector evolution via multispecies interbreeding and retargeting of adeno-associated viruses. *J. Virol.* **82,** 5887–5911 (2008).
42. Atasoy, D., Aponte, Y., Su, H. H. & Sternson, S. M. A. FLEX switch targets Channelrhodopsin-2 to multiple cell types for imaging and long-range circuit mapping. *J. Neurosci.* **28,** 7025–7030 (2008).
43. Tsai, H. C. *et al.* Phasic firing in dopaminergic neurons is sufficient for behavioral conditioning. *Science* **324,** 1080–1084 (2009).
44. Mebatsion, T., Konig, M. & Conzelmann, K. K. Budding of rabies virus particles in the absence of the spike glycoprotein. *Cell* **84,** 941–951 (1996).
45. Wickersham, I. R., Sullivan, H. A. & Seung, H. S. Production of glycoprotein-deleted rabies viruses for monosynaptic tracing and high-level gene expression in neurons. *Nature Protocols* **5,** 595–606 (2010).
46. Wolfart, J., Neuhoff, H., Franz, O. & Roeper, J. Differential expression of the small-conductance, calcium-activated potassium channel SK3 is critical for pacemaker control in dopaminergic midbrain neurons. *J. Neurosci.* **21,** 3443–3456 (2001).